

Superconductivity in electron-doped cuprates: Gap shape change and symmetry crossover with doping

Francisco Guinea,¹ Robert S. Markiewicz,² and María A. H. Vozmediano³

¹*Instituto de Ciencia de Materiales de Madrid, CSIC, Cantoblanco, E-28049 Madrid, Spain*

²*Physics Department, Northeastern University, Boston, Massachusetts 02115, USA*

³*Departamento de Matemáticas, Universidad Carlos III de Madrid, 28911 Leganés, Madrid, Spain*

(Received 3 February 2003; revised manuscript received 2 October 2003; published 27 February 2004)

The Kohn-Luttinger mechanism for superconductivity is investigated in a model for the electron-doped cuprates. The symmetry of the order parameter of the superconducting phase is determined as a function of the geometry of the Fermi surface together with the structure of the electron-hole susceptibility. It is found to remain $d_{x^2-y^2}$ wave within a large doping range. The *shape* of the gap anisotropy evolves with doping, with the maximum gap moving away from $(\pi,0)$, in good agreement with recent experiments. As the shift of the maximum increases, a crossover to d_{xy} symmetry is found.

DOI: 10.1103/PhysRevB.69.054509

PACS number(s): 71.10.Fd, 74.20.-z

I. INTRODUCTION

The single-band Hubbard model with longer-range hoppings—(t - t') Hubbard model—is being widely accepted as a minimal model to describe the physics of the high- T_c cuprates.¹ It gives most of the qualitative aspects of the phase diagram: antiferromagnetism near half filling, superconductivity, pseudogap, and striped phases. The greatest effort has previously been centered in understanding hole-doped compounds as they possess the highest available T_c . The complication of the phase diagram in the underdoped to optimally doped regimes, partially due to the inhomogeneous structures and the proximity of the Van Hove singularity, has recently renewed interest in electron-doped compounds.²

Although the estimated values of the Hubbard interaction U lie in the intermediate regime, most of the previous features can be obtained in the weak-coupling limit which has the advantage of often permitting analytical computations where the physics is more transparent.

Superconductivity has been obtained in the purely repulsive model with quantum Monte Carlo³ and other numerical methods,⁴ with the antiferromagnetic fluctuation exchange approximation,⁵⁻⁷ and with renormalization-group methods in the proximity of the Van Hove singularity.⁸ At present there is no general agreement on the mechanism for superconductivity. As for the symmetry of the superconducting order parameter, it is generally assumed to be d wave in the hole-doped cuprates and remains unclear in the electron-doped compounds.⁹

One of the most physically appealing mechanisms for obtaining a pairing instability from repulsive interactions goes back to Kohn and Luttinger¹⁰ (KL), who demonstrated the instability of a three-dimensional (3D) isotropic Fermi system towards pairing due to the spatial modulation of the effective interaction at a wave vector of $2k_F$. The KL mechanism has been extended to other electron systems and dimensions¹¹⁻¹³ and has been extensively studied in the 2D Hubbard model.¹⁴⁻¹⁷ The Kohn-Luttinger mechanism has very recently been reanalyzed in Ref. 18.

In the study of the instabilities of an electron system a

principal role is played by the electron-hole susceptibility $\chi(\vec{k},\omega)$ whose imaginary part measures the density of electron-hole pairs with energy ω and whose real part renormalizes the scattering amplitude. Scattering processes which involve opposite points of the Fermi surface can be enhanced by its special geometry (nesting and Van Hove singularities are extreme examples), or by other physical features.

In Ref. 19, a scaling analysis was used to study the pairing instabilities of a general Fermi surface in the 2D square lattice as a function of its geometry. It was shown that the curvature of the Fermi line modulates the effective interaction in the BCS channel in such a way that different harmonics scale as different powers of the scaling parameter. As the latter goes to zero some harmonics become negative giving rise to a KL superconductivity in the given channel.

In this paper we will perform a KL analysis of electron-doped cuprates along the lines of Ref. 19 based on special features of the susceptibility. Recent experiments on electron-doped cuprates⁹ propose a change in the symmetry of the superconducting order parameter from d wave below and around optimal doping to s wave in the overdoped regime. Moreover, even when the gap has overall d -wave symmetry, its angle dependence evolves with doping, picking up substantial harmonic content for hole underdoping, and there is some evidence²⁰ that the peak shifts away from $(\pi,0)$ in electron-doped cuprates. This issue will also be studied in the paper.

The organization is as follows. In Sec. II we set the model, review the main arguments of the scaling analysis of Ref. 19, and establish the d -wave nature of the superconducting phase. In Sec. III we analyze the structure of the spin susceptibility to be used in the calculation. Section IV is devoted to the evolution of the symmetry of the order parameter with doping followed by our conclusions.

II. THE MODEL AND KOHN-LUTTINGER MECHANISM

The Fermi surface of the electron compounds for the doping values of interest has a general rounded shape centered at (π,π) with flatter portions in the diagonal directions. The

t - t' Hubbard model with negative values of t' is the simplest model that reproduces the observed feature. The dispersion relation is given by

$$\epsilon(\vec{k}) = -2t(\cos k_x + \cos k_y) - 4t' \cos k_x \cos k_y. \quad (1)$$

For definiteness we assume $t = 0.326$ eV, $t'/t = -0.276$ in our calculations.^{21–24}

The Kohn-Luttinger mechanism is closely related to Friedel oscillations. It is well known that, due to the sharp cutoff of the electron distribution in k space at the Fermi level, impurity potentials in a metal do not fall off monotonically but have a superposed (Friedel) oscillation. Kohn and Luttinger showed that a similar oscillation arises in the electron-electron interaction, leading to an *attractive* interaction between two electrons separated by the right distance—the position of the first Friedel minimum. In turn, the attractive interaction can lead to a superconducting instability.

The calculation can readily be formulated in renormalization-group language,²⁵ based on the fact that the effective coupling constants of a given Hamiltonian (vertex functions) acquire an energy-momentum dependence upon renormalization behaving like effective potentials. In the simplest Fermi-liquid model (gas of electrons with spherical Fermi surface and short-range four Fermi interactions), only the forward and BCS channels get renormalized.²⁵ The standard KL mechanism occurs when the effective BCS vertex at a given momentum ($2k_F$) oscillates in such a way that some of its Fourier components become negative. The system then undergoes a superconducting transition. The symmetry of the superconducting order parameter can be found by expanding the potential in eigenfunctions of the symmetry of the model (spherical harmonics in the spherical case) and finding the lowest negative eigenvalue.

This is the analysis that we will follow in Sec. IV of the paper adapted to case the Fermi surface given by the contour lines of Eq. (1).

The KL mechanism for the rounded Fermi surface corresponding to electron-doped cuprates was analyzed in Ref. 19 and shown to induce a pairing instability with $d_{x^2-y^2}$ symmetry without special features of the susceptibility. Based on very simple scaling arguments, it was shown that the electron susceptibility is proportional to $(1/f^2)$, where f is the curvature of the Fermi surface and gets modulated by it. Hence it has maxima for the scattering vectors joining two opposite points of the Fermi surface in the $(\pi/2, \pi/2)$ direction and equivalent points where the curvature reaches its minimum value. It has minima in the zero and equivalent directions. This situation corresponds to $d_{x^2-y^2}$ symmetry. This analysis is independent of the specific form of the spin susceptibility. The detailed study of the susceptibility in the following section reinforces the symmetry arguments of Ref. 19 and the d -wave character of the instability.

III. THE STRUCTURE OF THE SPIN SUSCEPTIBILITY

Recent angle-resolved photoemission spectroscopy (ARPES) of electron-doped $\text{Nd}_{2-x}\text{Ce}_x\text{CuO}_{4\pm\delta}$ (Ref. 2) found a smooth evolution of the band dispersion with dop-

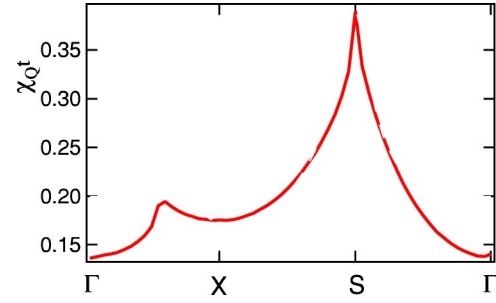


FIG. 1. Bare susceptibility at the termination of the plateau described in the text, $\mu = 0$. Brillouin-zone points are $\Gamma = (0,0)$, $X = (\pi,0)$, $S = (\pi,\pi)$.

ing, from half filling to optimal doping, which could be interpreted²⁶ in terms of the gradual filling of the upper Hubbard band. Doping gradually reduces the Mott gap that closes near optimal doping. This doping also falls close to another interesting point²⁷ where the displaced Fermi surface is tangent to the original one and the susceptibility χ at $\vec{Q} = (\pi, \pi)$ starts to drop precipitously.

Near this point, the magnetic susceptibility has the form of a nearly flat-topped plateau in momentum space, with sharp falloff away from the plateau. The plateau is defined by the presence of points at which the Fermi surface (FS) overlaps the FS image shifted by \vec{Q} . If the FS image is shifted away from \vec{Q} by an additional \vec{q}' , then for some critical value $\vec{q}' = \vec{q}_c$, one or more of the overlaps ceases to exist as the two FS's pull apart. The value of q_c , which defines the plateau boundary in a given direction, satisfies

$$-2t[\sin(q_x/2) + \sin(q_y/2)] - 4t' \sin(q_x/2) \sin(q_y/2) = \mu, \quad (2)$$

where μ is the chemical potential.

The plateau exists in the doping range $0 \geq \mu \geq \mu_{VHS} = 4t'$, where μ_{VHS} is the doping of the Van Hove singularity (VHS). When $\mu = 0$, the width of the plateau shrinks to zero. The plateau approximately satisfies the form $\chi = A - B\Theta(q' - q_c)\sqrt{q' - q_c}$, with Θ a step function. As the width of the plateau vanishes $q_c \rightarrow 0$, the two square-root terms merge at a single point. The resulting susceptibility is depicted in Fig. 1. We find that the *angle dependence* of the resulting superconducting gap function changes dramatically depending on whether the doping lies on or off of this susceptibility plateau (leading ultimately to changes in the gap *symmetry*).

At $T = 0$, the susceptibility $\chi_{\vec{q}}$ can be written as

$$\begin{aligned} \chi_{\vec{q}} &= \int \frac{d^2\vec{k}}{(2\pi)^2} \frac{1}{(\epsilon_{\vec{k}+\vec{q}} - \epsilon_{\vec{k}})} \\ &= \frac{1}{2t} \int \frac{d^2\vec{k}}{(2\pi)^2} \\ &\quad \times \frac{1}{(\cos(k_x + q_x) + \cos(k_y + q_y) - \cos k_x - \cos k_y)}. \end{aligned} \quad (3)$$

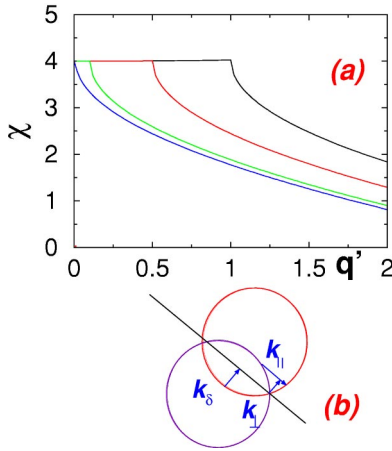


FIG. 2. (a) Calculated susceptibility $\chi(q)$ for several values of overlap k_δ (from right to left, $k_\delta/q=0.5, 0.25, 0.05$, and 0, the last corresponding to the termination of hot spot overlap). (b) Schematic of Fermi surfaces, defining k_δ , k_\perp , and k_\parallel .

The Fermi functions limit the integral to a sum of approximately wedge-shaped areas. We begin at the antiferromagnetic wave vector $\vec{q} = \vec{Q} = (\pi, \pi)$. Letting $k_i = \pi/2 + k'_i$, $i = x, y$, then to lowest order the energy becomes

$$\epsilon_{\vec{k}} = 2\sqrt{2}tk'_\perp + 2t'k'_\parallel{}^2, \quad (4)$$

with k_\parallel and k_\perp the momenta parallel and perpendicular to the zone diagonal (magnetic Brillouin-zone boundary). Linearizing the energy denominator, $\Delta \epsilon \propto k_\perp$, independent of k_\parallel ,

$$\chi_{\vec{Q}} \approx \frac{1}{8\pi^2\sqrt{2}t} \int_0^{k_c} \frac{dk_\perp dk_\parallel}{k_\perp} = \frac{I}{4\pi^2 t}. \quad (5)$$

The FS centered at (π, π) and the Q -shifted FS are illustrated schematically in Fig. 2(b). The region of integration is over the part of the upper FS in Fig. 2(b) not overlapped by the lower (Q -shifted) FS, and k_\perp ranges from 0 at the apex of the wedge to $k_c = k_F - k_\delta$ at the middle of the upper FS, where k_F is the radius of the FS and k_δ is the overlap parameter defined in Fig. 2(b). Assuming $k_\delta \ll k_F$ and keeping only the lowest-order contributions,

$$\begin{aligned} I &= \sqrt{k_F} \left[\int_0^{k_c} dk_\perp \frac{\sqrt{k_\perp + k_\delta}}{k_\perp} - \int_0^{k_\delta} dk_\perp \frac{\sqrt{k_\delta - k_\perp}}{k_\perp} \right] \\ &= 2k_F + \sqrt{k_F k_\delta} \ln \left| \frac{1 - \beta}{1 + \beta} \right|, \end{aligned} \quad (6)$$

with $\beta = \sqrt{k_\delta/k_F}$. For the q -dependent susceptibility, let $\vec{q} = \vec{Q} + \vec{q}'$. Then the FS is shifted by \vec{q}' , or $k_\delta \rightarrow k_\delta + q'/2$ for the surface shown, $k_\delta \rightarrow k_\delta - q'/2$ for the FS at $(-\pi, -\pi)$, so $\chi_q \propto I_{k_\delta + q'/2} + I_{k_\delta - q'/2}$. There is one correction. For $q' > 2k_\delta$, the two FS's no longer overlap, and the integral runs over the full half-circle, but k_\perp is measured from halfway between the two FS's, so $I_{k_\delta - q'/2} = 2k_F [1 - \gamma \tan^{-1} 1/\gamma]$, with $\gamma = \sqrt{(q' - 2k_\delta)/2k_F}$. Figure 2(a) shows the resulting susceptibilities for several values of k_δ . The calculation ex-

plains the very flat top with weak positive curvature and the sharp falloff at $q' = 2k_\delta$. For increased electron doping, the holelike Fermi surface shrinks, $k_\delta \rightarrow 0$, and the plateau width shrinks to zero. Near the plateau edge $\chi \sim 1 - \pi\gamma/2$ varies as $\sqrt{q'}$. The cusplike susceptibility in Fig. 2(a) at the point where the plateau terminates corresponds to the χ_0 peak in Fig. 1 at $S = (\pi, \pi)$. With the assumed parameter values, this happens when $\mu = 0$, corresponding to an electron doping $x \approx -0.19$; on the hole doped side, the plateau terminates when $\mu = 4t' = -0.359$ eV, at a hole doping, $x = 0.24$.

IV. COUPLING-CONSTANT CALCULATIONS

Calculation of the *magnitude* of the superconducting transition gap is beyond the scope of the present paper. This requires a better understanding of (a) the proper choice of susceptibility, (b) incorporation of the frequency dependence of the susceptibility, (c) proper accounting of the competition with magnetic ordering, and (d) solution of the resulting (generalized) Eliashberg equations.

The most negative coupling constant determines the dominant gap symmetry, while the corresponding eigenfunction gives the angle dependence of the gap.

In this section we investigate the possible change in the symmetry of the superconducting order parameter and how its angle dependence evolves with doping.²⁰

The pairing coupling constant in a given symmetry sector is given by the matrix^{6,17}

$$\lambda_{n,m}^\alpha = \frac{1}{(2\pi)^2} \int \frac{d\mathbf{k}}{v_k} \int \frac{d\mathbf{k}'}{v_{k'}} V(\mathbf{k}, \mathbf{k}') \Delta_{an}(\mathbf{k}) \Delta_{am}(\mathbf{k}'). \quad (7)$$

where $V(\mathbf{k}, \mathbf{k}') = U + U^2 \chi(\mathbf{k} + \mathbf{k}')$ and $\Delta_{an}(\mathbf{k})$ is the normalized $[\int d\mathbf{k}/v_k \Delta_{am} \Delta_{an}(\mathbf{k}) = \delta_{mn}]$ weight function expanded in terms of the irreducible representations h_{an} of the symmetry group. We approximate the CuO_2 plane by a square lattice, in which case the appropriate symmetry group is D_4 , for which there are four singlet and one doublet representations. These representations define gap symmetry sectors: While Eq. (7) can mix basis functions *within* a given sector, it does not mix functions *between* sectors. The four singlet sectors are labeled according to their lowest basis functions, as s , d (for $d_{x^2-y^2}$), d_{xy} , and g , while the doublet sector is labeled p —actually, there are two subsectors p_x and p_y which do not mix, but have degenerate eigenvalues. The corresponding basis functions are (with n ranging from 0 to ∞)

$$h_{s,n}(\phi) = \cos[4n\phi],$$

$$h_{d,n}(\phi) = \cos[(4n+2)\phi],$$

$$h_{d_{xy},n}(\phi) = \sin[(4n+2)\phi],$$

$$h_{g,n}(\phi) = \sin[4(n+1)\phi],$$

$$h_{p_x,n}(\phi) = \sin[(2n+1)\phi],$$

$$h_{p_y,n}(\phi) = \cos[(2n+1)\phi]. \quad (8)$$

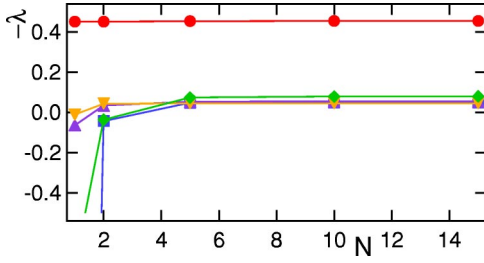


FIG. 3. Development of coupling constant with increasing matrix size N for $\mu = -0.1$ eV. Circles, $d_{x^2-y^2}$; up-pointing triangles, g ; diamonds, p_x ; squares, s ; and down-pointing triangles, d_{xy} .

The above functions describe the orbital symmetry—the singlet (doublet) representations corresponding to spin singlets (triplets). Below, we evaluate the *lowest* eigenvalue for each symmetry sector and label the corresponding eigenfunction by the sector—even though, e.g., the lowest s -wave solution is really an “extended- s ” solution, with all the $h_{s,n}$, $n > 0$, orthogonal to the pure s -wave solution.

For $\mu \leq \mu_{VHS}$, the Fermi surface is an electronlike Fermi surface closed about the Γ point $(0,0)$, and the angle ϕ must be measured about this point. For $\mu \geq \mu_{VHS}$, the topology of the Fermi surface changes to holelike, centered on (π, π) , and ϕ must now be measured from this point.

The maximal superconducting coupling is given by the minimal (i.e., maximally negative) eigenvalue of the λ matrix, Eq. (7). To solve this equation, the matrix was cut off at a finite size $N \times N$, with $N = 15$. This large N value was employed to assure adequate convergence in all sectors. This is illustrated in Fig. 3. If the $N = 1$ eigenvalue is already negative, the only change with N is a small increase in magnitude (due to level repulsion). But if the $N = 1$ eigenvalue is positive, N plays a larger role. There are two effects: first, a diagonal matrix element might itself be negative and, second, level repulsion always pushes the largest and smallest eigenvalues away from the mean. For example, for the s -wave sector, all the diagonal elements are found to be positive, but level repulsion generally leads to a small negative eigenvalue. However, for the parameter range studied, this is always too weak to be of interest.

The results of the analysis are shown in Fig. 4 for a variety of dopings (for electron doping x is considered negative), assuming $U = 6t$. Reasonable λ values are found for both electron and hole doping, but do not include the suppression of superconductivity near half filling caused by the magnetic order. While λ decreases with electron doping, the preferred symmetry remains $d_{x^2-y^2}$ over the doping range of interest. The present calculation thus provides no indication for a d to s crossover of the symmetry. However, at a higher doping, $x \sim -0.39$, there is a crossover from $d_{x^2-y^2}$ to d_{xy} symmetry; near such a crossover, there is likely to be a range of (gapless) $d_{x^2-y^2} + id_{xy}$ symmetry,²⁸ which may simulate an s -wave gap. Alternatively, the symmetry change may be associated with an additional pairing contribution due to electron-phonon coupling. It is interesting to see that d -wave symmetry is dominant at both sides of half filling, as found experimentally.

The Van Hove instability is clearly noticeable as the (di-

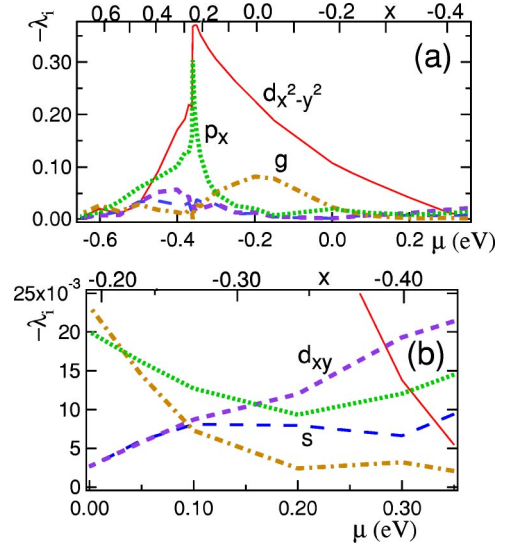


FIG. 4. (a) Evolution of the superconducting effective coupling as a function of doping, for a variety of gap symmetries: solid line, $d_{x^2-y^2}$; dot-dashed line, g ; dotted line, p_x ; long dashed, s ; short dashed, d_{xy} . (b) Blowup of electron doping.

vergent) peak in the holelike sector. However, for superconductivity, the relevant parameter is likely to be λ/Z , Fig. 5, where $Z = 1 + \lambda_s$ and λ_s is the $(0,0)$ matrix element in the s -wave sector of Eq. (7) (note that this is the only term which includes the linear-in- U contribution to V). This renormalization eliminates the Van Hove peak, shifting the largest d -wave gap to a lower hole doping. This is quite suggestive of the experimental situation, where there appears to be a quantum critical point somewhat above optimal hole doping,²⁹ which may be associated with the VHS.²⁷

We find a striking evolution of the *angular dependence* of the d -wave gap, as shown in Fig. 6. The Kohn-Luttinger mechanism leads to significant harmonic admixture, which changes as a function of doping. Including all harmonics, the gap functions contain excessive structure, so the following approximation was introduced, to provide smoother and more robust gap functions. For each added harmonic order [going from an $N \times N$ to an $(N+1) \times (N+1)$ matrix], the change in the smallest (largest negative) eigenvalue was monitored, and if the fractional change was less than some small reference value α (typically, $\alpha = 0.02$ was used), the coupling to this harmonic was neglected. This reduced the matrix problem from 15×15 to $N \times N$, where N was generally 2–4, except in the immediate vicinity of the Van Hove

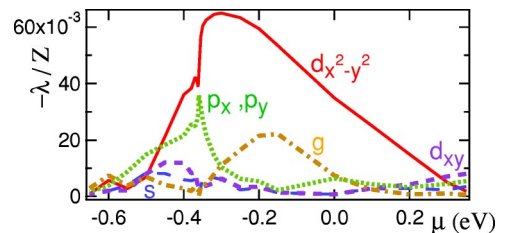


FIG. 5. Normalized coupling constants λ/Z for same data as in Fig. 4.

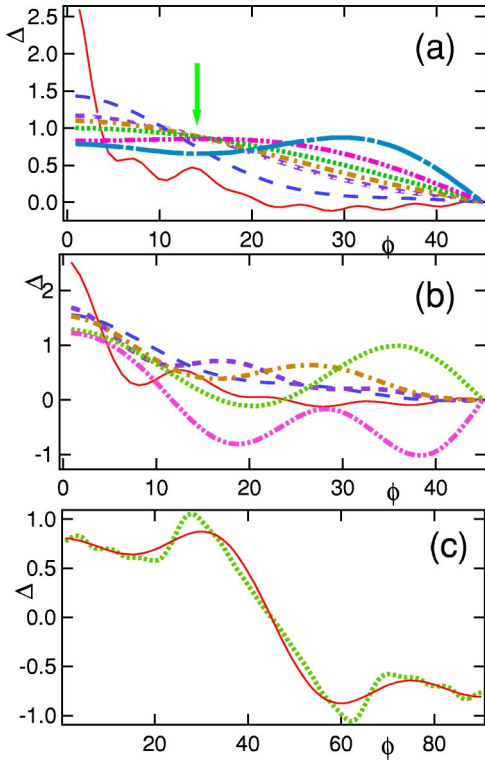


FIG. 6. (a) Angular dependence of the superconducting gap for the d -wave symmetry solution, for several dopings: the chemical potentials [hole densities] are $\mu[x] = -0.3599$ eV [0.247] (thin solid line), -0.35 eV [0.22] (long dashed line), 0 eV [-0.19] (short dash-dotted line), 0.10 eV [-0.28] (dotted line), 0.20 eV [-0.35] (dash-dot-dotted line), and 0.3 eV [-0.41] (long dash-dotted line). Arrow, datum of Ref. 20. (b) Continuation to higher hole doping, with $\mu[x] = -0.3599$ [0.247] (thin solid line), -0.38 [0.30] (long dashed line), -0.4 [0.33] (short dashed line), -0.45 [0.41] (dot-dashed line), -0.5 [0.49] (dotted line), and -0.55 [0.55] (dash-dot-dotted line). (c) gap function for $\mu = 0.3$ eV, comparing a calculation employing all 15 harmonics (dotted line) with one involving only the dominant four harmonics (solid line).

singularity, where more harmonics were needed. An example is shown in Fig. 6(c), while Figs. 6(a,b) show only smoothed data, except at the VHS, where all harmonics are shown in Fig. 6(a), and only the dominant $N=7$ in Fig. 6(b).

For all hole dopings the peak stays close to $(\pi, 0)$, but harmonic content tends to sharpen the peak and flatten Δ near the nodes, deviating from the simplest $\cos k_x - \cos k_y$ form. Such flattening has been found in both ARPES (Refs. 30 and 31) and scanning tunneling microscopy³² experiments. However, the experimental trend is that the harmonic content is enhanced in underdoped samples,³³ whereas the calculated trend is for larger harmonic content to develop near the VHS—i.e., with increasing hole doping. [In comparing to experiment, it must be kept in mind that, for $\mu > -0.3599$ eV, all angle ϕ measurements are centered at (π, π) , with $\phi=0$ corresponding to $(\pi, 0)$.]

As the doping shifts toward electronlike, there is a significant shift of the peak position with ϕ , away from $(\pi, 0)$. This result is consistent with recent observations by Blum-

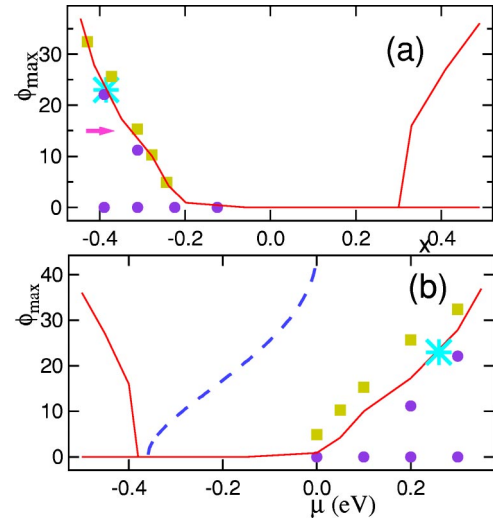


FIG. 7. Shift of $d_{x^2-y^2}$ peak from $(\pi, 0)$ as a function of doping (a) and chemical potential (b). The filled circles (squares) correspond to changing t' to $-0.12t$ ($-0.425t$); the dashed line in (b) is the position of the hot spots. Arrow in (a), datum of Ref. 20. Asterisk, point of crossover to d_{xy} symmetry.

berg *et al.*²⁰ (One should, however, note the debate.^{34,35}) However, the agreement is not quantitative: a shift of the peak to $\sim 15^\circ$ is found for an experimental doping of $x = -0.15$, whereas the predicted doping is -0.32 , Fig. 7. Indeed, there appears to be a close correlation between the shift of the d -wave peak and the crossover of the symmetry from $d_{x^2-y^2}$ to d_{xy} : the crossover occurs when the peak has shifted about halfway to 45° (asterisk in Fig. 7). Note that a similar shift arises on the hole-overdoped side, although a second, larger peak remains at $\phi = 0$.

This shift of the peak from $(\pi, 0)$ does not follow the position of the hot spots on the Fermi surface [dashed line in Fig. 7(b)], but depends on whether or not the system is on the susceptibility plateau. The peak stays close to $(\pi, 0)$ as long as the chemical potential is on the hot spot plateau ($\mu < 0$), then rapidly shifts toward 45° . Similarly, for $\mu < -0.3599$ eV (off of the other side of the plateau, beyond the VHS), a second peak appears and shifts to 45° by $\sim \mu = -0.5$, Fig. 6(b), by which point the gap has crossed over to p -wave symmetry.

For the electron-doping case we have studied how this peak shift changes when the plateau width (or τ) is varied. From Eq. (7) the angle dependence is controlled by the product of two terms, a weighted density of states, $g(\mathbf{k}) = \Delta_{s,1}(\mathbf{k})k^2(\phi)/v_k$, and a weighted susceptibility $\bar{V}(\mathbf{k}) = \int d\phi' V(\mathbf{k}, \mathbf{k}')g(\mathbf{k}')$. The latter $\bar{V}(\mathbf{k})$ peaks at $(\pi, 0)$ on the plateau, and starts shifting toward 45° as soon as μ is off of the plateau. However, $g(\mathbf{k})$ continues to peak at $(\pi, 0)$, and the product shifts off of $(\pi, 0)$ more slowly as τ is reduced.

In conclusion by rather general symmetry arguments we have shown that d -wave superconductivity is a robust feature of the cuprates both hole and electron doped. We have also examined the evolution of the shape of the order parameter with doping and found a deviation of the order parameter

angle dependence from simple $\cos 2\phi$ form similar to that measured in recent experiments (Fig. 4). Although the calculations are based on a weak-coupling analysis we believe that they are justified in the electron-doped case, and that more refined computations will not change the general features.

Note added. Recently, we became aware of a similar calculation.³⁶ Here, a doping-independent nearly antiferromagnetic Fermi-liquid susceptibility was introduced in place of the lowest-order (Kohn-Luttinger) form we assumed. A very similar crossover of gap symmetry with electron doping was found, with two differences. First, the crossover was found to be at the doping at which the hot spot plateau terminated. This is probably not very significant, however: the parameters are so different that this actually corresponds to a higher doping ($x \sim -0.59$) than we found, and much higher than in the experiments. More significant is that we find a

crossover from $d_{x^2-y^2}$ to d_{xy} symmetry, while their crossover is to p -wave symmetry. We have repeated our calculations using the full self-consistent susceptibility,²⁷ and find for this nearly divergent susceptibility that the crossover is to a state of either p - or g -wave symmetry. These results will be reported in a future publication.

ACKNOWLEDGMENTS

The financial support of the CICyT (Spain), through Grants Nos. PB96-0875, 1FD97-1358, and BFM2000-1107 is gratefully acknowledged. One of us (R.M.) has been supported by the Spanish Ministerio de Educación through Grant No. SAB2000-0034.

- ¹P.W. Anderson, *Science* **235**, 1196 (1987); cond-mat/0201429 (unpublished).
- ²N.P. Armitage, F. Ronning, D.H. Lu, C. Kim, A. Damascelli, K.M. Shen, D.L. Feng, H. Eisaki, Z.-X. Shen, P.K. Mang, N. Kaneko, M. Greven, Y. Onose, Y. Taguchi, and Y. Tokura, *Phys. Rev. Lett.* **88**, 257001 (2002).
- ³D.J. Scalapino and S.R. White, *Found. Phys.* **31**, 27 (2001); S. Sorella, G.B. Martins, F. Becca, C. Gazza, L. Capriotti, A. Parola, and E. Dagotto, *Phys. Rev. Lett.* **88**, 117002 (2002).
- ⁴Th. Maier, M. Jarrell, Th. Pruschke, and J. Keller, *Phys. Rev. Lett.* **85**, 1524 (2000); A. Paramekanti, M. Randeria, and N. Trivedi, *ibid.* **87**, 217002 (2001); M. Ogata and A. Himeda, *J. Phys. Soc. Jpn.* **72**, 374 (2003).
- ⁵K. Miyake, S. Schmitt-Rink, and C.M. Varma, *Phys. Rev. B* **34**, 6554 (1986).
- ⁶D.J. Scalapino, E. Loh, Jr., and J.E. Hirsch, *Phys. Rev. B* **34**, 8190 (1986); **35**, 6694 (1987).
- ⁷N.E. Bickers, D.J. Scalapino, and S.R. White, *Phys. Rev. Lett.* **62**, 961 (1989).
- ⁸J.V. Alvarez, J. González, F. Guinea, and M.A.H. Vozmediano, *J. Phys. Soc. Jpn.* **67**, 1868 (1998); J. González, F. Guinea, and M.A.H. Vozmediano, *Phys. Rev. Lett.* **84**, 4930 (2000).
- ⁹See, for instance, A. Biswas, P. Fournier, M.M. Qazilbash, V.N. Smolyaninova, H. Balci, and R.L. Greene, *Phys. Rev. Lett.* **88**, 207004 (2002), and references therein.
- ¹⁰W. Kohn and J.M. Luttinger, *Phys. Rev. Lett.* **15**, 524 (1965).
- ¹¹M.Yu. Kagan and A.V. Chubukov, *Pis'ma Zh. Eksp. Teor. Fiz.* **47**, 525 (1988) [*JETP Lett.* **47**, 614 (1988)].
- ¹²M.A. Baranov, M.Yu. Kagan, and A. Chubukov, *Int. J. Mod. Phys. B* **6**, 2471 (1992).
- ¹³A.V. Chubukov, *Phys. Rev. B* **48**, 1097 (1993).
- ¹⁴M.A. Baranov and M.Yu. Kagan, *Z. Phys. B: Condens. Matter* **86**, 237 (1992).
- ¹⁵A.V. Chubukov and J.P. Lu, *Phys. Rev. B* **46**, 11 163 (1992).
- ¹⁶D. Zanchi and H.J. Schulz, *Phys. Rev. B* **54**, 9509 (1996).
- ¹⁷R. Hlubina, *Phys. Rev. B* **59**, 9600 (1999).
- ¹⁸V.M. Galitski and S. Das Sarma, *Phys. Rev. B* **67**, 144520 (2003).
- ¹⁹J. González, F. Guinea, and M.A.H. Vozmediano, *Phys. Rev. Lett.* **79**, 3514 (1997); *Int. J. Mod. Phys. B* **13**, 2545 (1999).
- ²⁰G. Blumberg, A. Koitzsch, A. Gozar, B.S. Dennis, C.A. Kendziora, P. Fournier, and R.L. Greene, *Phys. Rev. Lett.* **88**, 107002 (2002).
- ²¹These parameters have been found to fit the electronic dispersion in undoped (Ref. 22) and electron-doped (Ref. 26) cuprates, while very similar parameters fit the spin-wave dispersion (Refs. 23 and 24) in La_2CuO_4 .
- ²²R.S. Markiewicz, *Phys. Rev. B* **62**, 1252 (2000).
- ²³N.M.R. Peres and M.A.N. Araújo, *Phys. Status Solidi B* **236**, 523 (2003).
- ²⁴H.M. Rønnow, D.F. McMorrow, R. Coldea, A. Harrison, I.D. Youngson, T.G. Perring, G. Aeppli, O. Syljuåsen, K. Lefmann, and C. Rischel, *Phys. Rev. Lett.* **87**, 037202 (2001).
- ²⁵J. Polchinsky, in *Proceedings of the 1992 TASI in Elementary Particle Physics*, edited by J. Harvey and J. Polchinski (World Scientific, Singapore, 1992); R. Shankar, *Rev. Mod. Phys.* **66**, 129 (1994).
- ²⁶C. Kusko, R.S. Markiewicz, M. Lindroos, and A. Bansil, *Phys. Rev. B* **66**, 140513 (2002).
- ²⁷R.S. Markiewicz, in *Intrinsic Multiscale Structure and Dynamics in Complex Electronic Oxides*, edited by A.R. Bishop, S.R. Shenoy, and S. Sridhar (World Scientific, Singapore, 2003), p. 109; cond-mat/0312594 (unpublished).
- ²⁸H. Ghosh, *Phys. Rev. B* **60**, 6814 (1999); M. Vojta, Y. Zhang, and S. Sachdev, *Phys. Rev. Lett.* **85**, 4940 (2000); Y. Dagan and G. Deutscher, *ibid.* **87**, 177004 (2001).
- ²⁹J.L. Tallon, J.W. Loram, G.V.M. Williams, J.R. Cooper, I.R. Fisher, J.D. Johnson, M.P. Staines, and C. Bernhard, *Phys. Status Solidi B* **215**, 531 (1999).
- ³⁰J. Mesot, M.R. Norman, H. Ding, M. Randeria, J.C. Campuzano, A. Paramekanti, H.M. Fretwell, A. Kaminski, T. Takeuchi, T. Yokoya, T. Sato, T. Takahashi, T. Mochiku, and K. Kadowaki, *Phys. Rev. Lett.* **83**, 840 (1999).
- ³¹A. Damascelli, Z.-X. Shen, and Z. Hussain, *Rev. Mod. Phys.* **75**, 473 (2003).
- ³²K. McElroy, R.W. Simmonds, J.E. Hoffmann, D.-H. Lee, J. Orenstein, H. Eisaki, S. Uchida, and J.C. Davis, *Nature (London)* **422**, 592 (2003).

- ³³S.V. Borisenko, A.A. Kordyuk, T.K. Kim, S. Legner, K.A. Nennkov, M. Knupfer, M.S. Golden, J. Fink, H. Berger, and R. Follath, *Phys. Rev. B* **66**, 140509 (2002).
- ³⁴F. Venturini, R. Hackl, and U. Michelucci, *Phys. Rev. Lett.* **90**, 149701 (2003).
- ³⁵G. Blumberg, A. Koitzsch, A. Gozar, B.S. Dennis, C.A. Kendziora, P. Fournier, and R.L. Greene, *Phys. Rev. Lett.* **90**, 149702 (2003).
- ³⁶V.A. Khodel, V.M. Yakovenko, M.V. Zverev, and H. Kang, *cond-mat/0307454* (unpublished).